Western Arctic Ocean temperature variability during the last 8000 years

Jesse R. Farmer,[1,2] Thomas M. Cronin,[1] Anne de Vernal,[3] Gary S. Dwyer,[4] Lloyd D. Keigwin,[5] and Robert C. Thunell[6]

Received 22 September 2011; revised 8 November 2011; accepted 9 November 2011; published 17 December 2011.

[1] We reconstructed subsurface (~200–400 m) ocean temperature and sea-ice cover in the Canada Basin, western Arctic Ocean from foraminiferal $\delta^{18}O$, ostracode Mg/Ca ratios, and dinocyst assemblages from two sediment core records covering the last 8000 years. Results show mean temperature varied from −1 to 0.5°C and −0.5 to 1.5°C at 203 and 369 m water depths, respectively. Centennial-scale warm periods in subsurface temperature records correspond to reductions in summer sea-ice cover inferred from dinocyst assemblages around 6.5 ka, 3.5 ka, 1.8 ka and during the 15th century Common Era. These changes may reflect centennial changes in the temperature and/or strength of inflowing Atlantic Layer water originating in the eastern Arctic Ocean. By comparison, the 0.5 to 0.7°C warm temperature anomaly identified in oceanographic records from the Atlantic Layer of the Canada Basin exceeded reconstructed Atlantic Layer temperatures for the last 1200 years by about 0.5°C. **Citation:** Farmer, J. R., T. M. Cronin, A. de Vernal, G. S. Dwyer, L. D. Keigwin, and R. C. Thunell (2011), Western Arctic Ocean temperature variability during the last 8000 years, *Geophys. Res. Lett.*, *38*, L24602, doi:10.1029/2011GL049714.

1. Introduction

[2] Studies of Arctic climate have revealed significant surface atmospheric warming [*Overland et al.*, 2004] and declines in sea-ice cover over the past few decades [*Comiso et al.*, 2008]. In addition, a 0.25 to 1°C warm temperature anomaly (WTA) in the subsurface Atlantic Layer (AL, 200-600 m water depth) reached the Canada Basin in the western Arctic Ocean from 1998 to 2007 [*Shimada et al.*, 2004; *McLaughlin et al.*, 2009]. Evidence for prior subsurface warming events during the 1950s and 1960s [*Swift et al.*, 2005] suggest they may represent a distinct mode of climate variability in the Arctic Ocean [*Polyakov et al.*, 2004, 2011]. Arctic instrumental records are sparse, however, and it is unclear to what degree the recent WTA represents natural variability or anthropogenic influence.

[3] Proxy records from sediment cores can provide evidence for large-scale natural variability in Arctic hydrography and sea-ice cover during the Holocene [*Keigwin et al.*, 2006; *Darby et al.*, 2009; *de Vernal et al.*, 2005; *McKay et al.*, 2008; *Polyak et al.*, 2009] against which recent changes can be compared. Here we reconstruct the first subsurface temperature records from the Atlantic Layer using stable isotopes ($\delta^{18}O$) and trace elements (Mg/Ca ratios), and sea-ice duration with dinocyst assemblages from two cores located in the Canada Basin on the Beaufort Sea continental margin.

2. Western Arctic Oceanography and Sediment Records

[4] The Atlantic Layer is composed of relatively warm (>0°C), saline (35 psu) North Atlantic water that enters the Arctic Ocean through the Fram Strait and Barents Sea, circulating counterclockwise along the shelf margins at intermediate depth [*Rudels et al.*, 2004] (Figure 1a). In the Western Arctic, cold (<0°C), relatively fresh (30–32 psu) Polar Mixed Layer (PML) water forms a surface layer (0–200 m) influenced by winter Bering Strait inflow water and upwelled AL water [*Woodgate et al.*, 2005]. A strong halocline and reverse thermocline separate the PML from the underlying AL where a temperature maximum (>0.5°C) occurs between 400 and 500 m. Core HLY0205-GGC19 (GGC-19) is located on the upper slope near Barrow Canyon at 369 m water depth within the AL, and core P1-92-AR-P1/B3 (piston and box cores, P1/B3) is from 203 m on the Chukchi Sea Shelf Edge within the base of the PML (Figure 1a, inset, and Figure 1b). Water in this region lies at the boundary of several oceanographic provinces [*Münchow and Carmack*, 1997] that are transformed by seasonal formation and melting of sea ice and atmospheric forcing [*Weingartner et al.*, 1998]. Chronostratigraphy for both cores was established using radiocarbon (^{14}C) dating, with average sedimentation rates of 65 cm kyr^{-1} for GGC-19 and ≥30 cm kyr^{-1} before 5.5 ka and after 1.5 ka in P1/B3 (auxiliary material).[1]

3. Temperature Proxies

[5] Oxygen isotopic composition ($\delta^{18}O$) of calcitic shells of two benthic foraminifera, *Islandiella helenae* and *Nonion labradoricum* in core GGC-19, and Mg/Ca ratios in the calcitic benthic ostracode *Krithe glacialis* in core P1/B3 were used for subsurface temperature reconstruction. Both $\delta^{18}O$ and Mg/Ca proxies are interpreted to represent mean

[1]U.S. Geological Survey, Reston, Virginia, USA.
[2]Now at Lamont-Doherty Earth Observatory, Earth Institute at Columbia University, Palisades, New York, USA.
[3]GEOTOP-UQAM-McGill, Montreal, Quebec, Canada.
[4]Division of Earth and Ocean Sciences, Nicholas School of the Environment, Duke University, Durham, North Carolina, USA.
[5]Woods Hole Oceanographic Institution, Woods Hole, Massachusetts, USA.
[6]Department of Earth and Ocean Sciences, University of South Carolina, Columbia, South Carolina, USA.

0094-8276/11/2011GL049714

[1]Auxiliary materials are available in the HTML. doi:10.1029/2011GL049714.

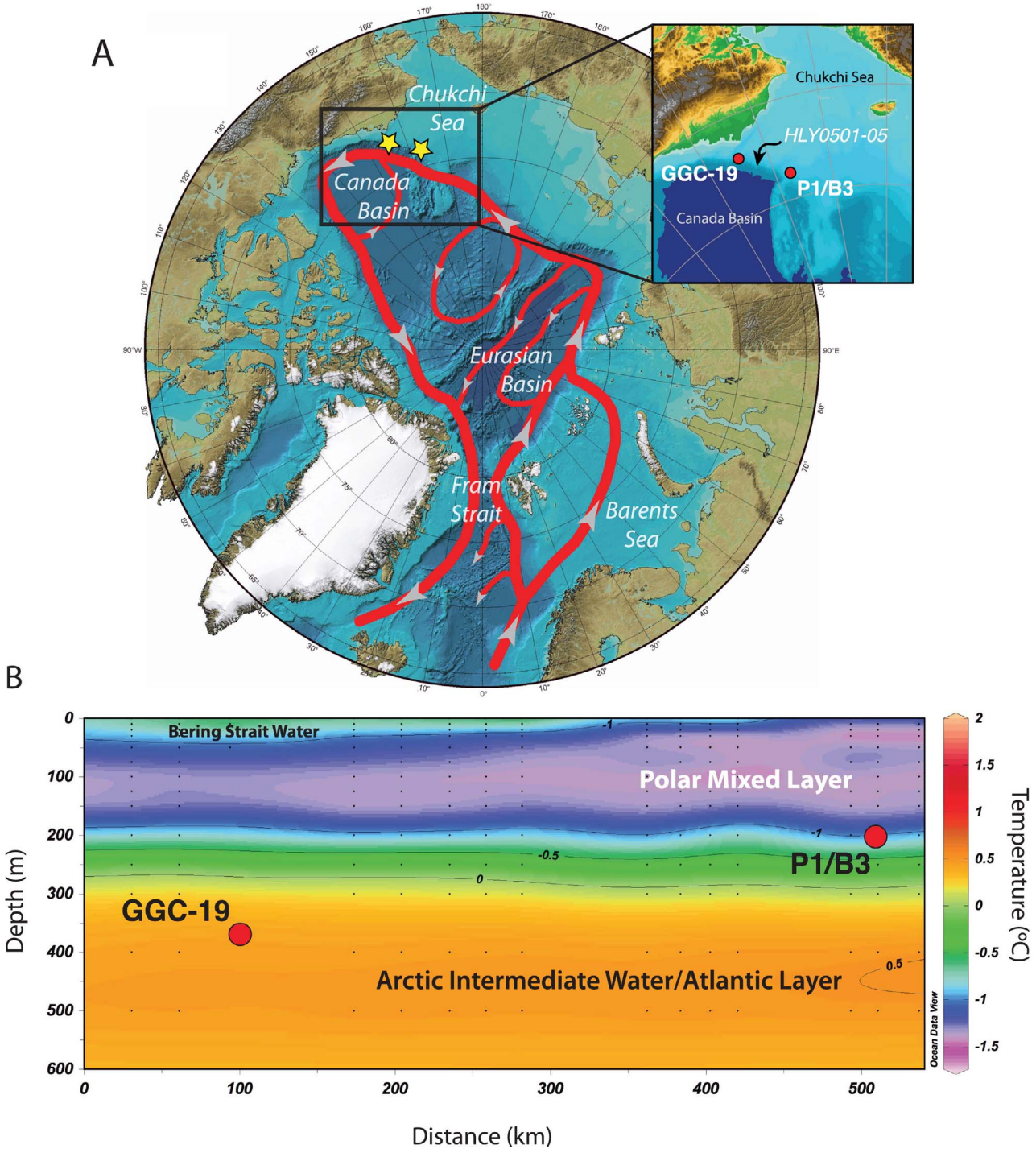

Figure 1. (a) Generalized circulation of the Atlantic Layer in the Arctic Ocean (from *Rudels et al.* [2004] and *de Vernal et al.* [2005]). Warm, saline North Atlantic water (red line) enters the Arctic at intermediate depths through the Fram Strait and Barents Sea before circulating counterclockwise (gray arrows) along the shelf margins and through the deep Arctic Basins. Yellow stars designate the two core sites. Base map and bathymetric data are from International Bathymetric Chart of the Arctic Ocean. Inset shows bathymetry near core sites GGC19 and P1/B3 (red circles), and the location of HLY0501-05 (black arrow). (b) East-west mean annual temperature profile across the Beaufort-Chukchi slope; core sites marked by red circles. Temperature data are from Polar Science Center Hydrographic Climatology (PHC, http://psc.apl.washington.edu/Climatology.html) plotted in Ocean Data View (http://odv.awi.de/) and predate the recent WTA. Temperature is contoured at 0.5°C intervals (black lines). Individual temperature measurements (black points) were interpolated to the shown gridded field using DIVA gridding with a 50 km × 40 m window.

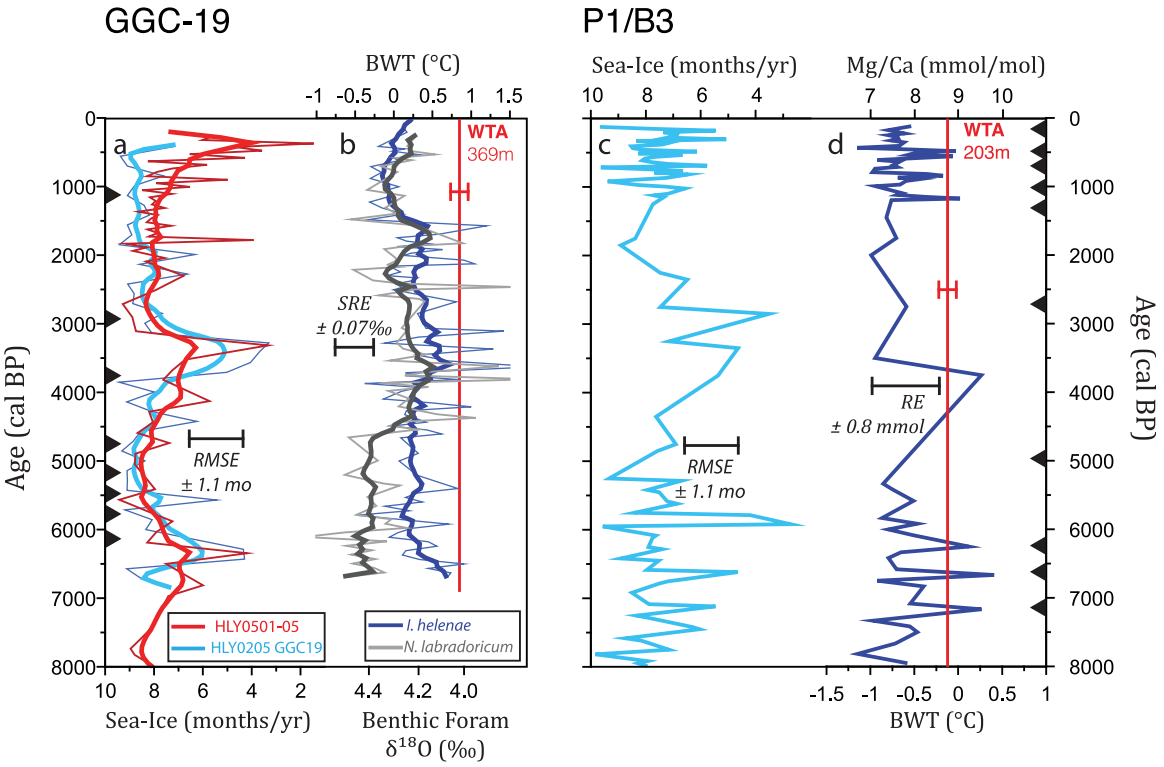

Figure 2. 8000-year Western Arctic temperature and sea-ice records. "(a) Sea-ice duration (months/year, axis reversed) from GGC19 (light blue) and HLY0501-05 (red) [*McKay et al.*, 2008]. (b) δ^{18}O from GGC19 for *I. helenae* (dark blue) and *N. labradoricum* (gray). Thick lines in (a) and (b) are 3 point smooths. (c) Unsmoothed sea-ice duration (axis reversed) and (d) *K. glacialis* ostracode Mg/Ca-based bottom water temperature for P1/B3; dinocyst sea-ice data adapted from *de Vernal et al.* [2005]. Black triangles denote radiocarbon dates for cores GGC-19 (Figure 2a) and P1/B3 (Figure 2d). Black bars in Figure 2a and Figure 2c denote the ± root mean square error (RMSE) of MAT-predicted sea-ice duration (1.1 months/year [*de Vernal et al.*, 2008]). Black bars in Figures 2b and 2d denote the ± relative error for δ^{18}O (3 point smooth) and Mg/Ca values as calculated from replicate analyses of samples and standards. Red line in Figure 2b and Figure 2d is the BWT reached during the WTA [*McLaughlin et al.*, 2009] at each respective core depth; the error on this measurement is estimated at ± 0.1°C (red bar).

annual subsurface temperature based on empirical calibrations [*Shackleton*, 1974; *Dwyer et al.*, 2002; *Cronin et al.*, 1996]. Although other factors can influence δ^{18}O and Mg/Ca ratios, we consider temperature the dominant cause of our observed variations (auxiliary material). Dinocyst assemblages are used to reconstruct past sea-ice patterns expressed as months of >50% sea-ice cover per year [*de Vernal et al.*, 2008]. Sea-ice duration for GGC-19 is supplemented by a sea-ice reconstruction from HLY0501-05 (415 m), proximally located along the Beaufort Sea slope within the AL [*McKay et al.*, 2008] (Figure 1a).

4. Results

[6] Sea-ice cover reconstructions from GGC-19 and HLY0501-05 generally track each other for the last 7 kyr (Figure 2a). δ^{18}O for *I. helenae* and *N. labradoricum* show similar patterns for the last 4 kyr, but *N. labradoricum* δ^{18}O is lower relative to *I. helenae* prior to 4.2 ka (Figure 2b). Reduced sea-ice duration from 7 ka to 6 ka, 3.8 to 3.0 ka and within the past 1 kyr is consistent with declines in *I. helenae* δ^{18}O in GGC-19 prior to 6 ka, between 4 and 2 ka, and within the past 1 kyr. During these intervals, 0.5 to 1°C warming of the AL implied from δ^{18}O corresponds with a ~25% decrease in yearly sea-ice duration. Average subsurface temperature for the last 7,000 years based on *I. helenae* δ^{18}O is 0.3°C, which is equivalent to AL temperatures prior to the recent warming [*McLaughlin et al.*, 2009].

[7] *Krithe glacialis* Mg/Ca and dinocyst records at the shallower P1/B3 site show multiple centennial-scale subsurface warming events of 1 to 1.5°C that coincide with periods of reduced sea-ice cover between 5.8 and 7.8 ka, and again during the last 1.5 kyr (Figures 2c and 2d). The lower sedimentation rate in P1/B3 between 1.5 and 5.2 ka precludes identification of submillennial variability but periods of surface and subsurface warmth at this site coincide with reduced sea-ice cover and increased AL temperature at GGC-19 before 6 ka and from 4.5 to 2.5 ka. Subsurface temperature maxima over the past 8 ka at P1/B3 are about 0.5°C warmer than temperatures at this depth during the 1998–2007 WTA.

[8] Focusing on the last 1,200 years, proxy records show evidence for temperature excursions during the Medieval Climate Anomaly (MCA, ~1000 to 1250 Common Era (CE)), the 15th century CE, and the Little Ice Age (LIA, ~1600-1800 CE) (Figure 3). Yearly sea-ice cover may have been reduced at P1/B3 during the MCA (Figure 3d), however there is no apparent change in sea-ice cover at GGC-19 or HLY0501-05, or in subsurface temperature at these sites. During the 15th century CE, subsurface temperature increa-

ses >1°C at P1/B3 and 0.5-0.75°C at GGC19, exceeding proxy measurement error and coinciding with reduced sea-ice duration at both locations, elevated SSTs in the Norwegian Sea (Figure 3e) [*Andersson et al.*, 2010], and the warmest pre-industrial conditions in the Arctic region of the past 1,000 years as indicated by terrestrial proxies and data-model simulations (Figure 3g) [*Crespin et al.*, 2009]. Post 15th century cooling evident in GGC-19 and P1/B3 correlates with lower SST on the Vøring Plateau, Norwegian Sea and cooler pan-Arctic atmospheric temperatures seen in terrestrial proxies. Our records agree with *Spielhagen et al.* [2011] in showing two periods of pre-anthropogenic warmth in the Arctic, although the absolute timing of these warm intervals is difficult to quantify due to age model uncertainty (Figure 3f). Nevertheless, it appears Atlantic Layer temperature during the WTA exceeded reconstructed subsurface temperature at site GGC-19 for the past 1,200 years by about 0.5°C (Figure 3a).

5. Discussion and Summary

[9] Proxy reconstructions of Holocene ocean temperature presented here demonstrate that the subsurface reverse thermocline characterizing the region today has existed in the western Canada Basin the last 7,000 years, with a cooler Polar Mixed Layer (203 m, mean −0.7°C) above a warmer Atlantic Layer (369 m, mean 0.3°C). Intervals of relatively warm AL water (1.0 to 1.5°C at GGC-19) appear to coincide both with increased temperature at the base of the PML (0 to 1°C at P1/B3) and times of reduced sea-ice cover. Concurrent warming in the AL and PML may be explained by increased upwelling of AL water to the halocline during WTA events, when both the temperature and volume of AL water are increased [*Woodgate et al.*, 2005; *McLaughlin et al.*, 2009]. Although our sediment records lack the resolution to identify decadal-scale, time-transgressive events like the WTA [*Polyakov et al.*, 2011], past periods of warm subsurface temperature might signify increased occurrence of WTA-like events over centennial timescales during the Holocene. The propagation of warm intrusions of the Atlantic Layer to the Canada Basin requires stability in the thermohaline structure of the water column provided by sea-ice cover [*McLaughlin et al.*, 2009]. A WTA-like mechanism to account for past warming events is consistent with evidence for perennial sea-ice cover in most regions of the Arctic for the last 5,000 years [*Cronin et al.*, 2010].

[10] Are western Arctic Ocean Holocene warming events manifestations of Arctic-wide climatic patterns? Holocene $\delta^{18}O$ variations in foraminifera of 0.25 to 0.5‰ from northern Barents Sea cores (460 m [*Lubinski et al.*, 2001] and 388 m [*Duplessy et al.*, 2001]) suggest 1-2°C changes in Atlantic water entering the Arctic. Paleoceanographic records from the southern Barents and Norwegian Seas indicate warming of AL source water during the 14th–15th centuries and abrupt cooling during the 16th century (Figure 3) [*Andersson et al.*, 2010], although surface processes such as sea-ice melt, coastal currents, productivity, and a shifting polar front may have influenced temperatures in these regions [*Hald et al.*, 2007; *Risebrobakken et al.*, 2010]. It is

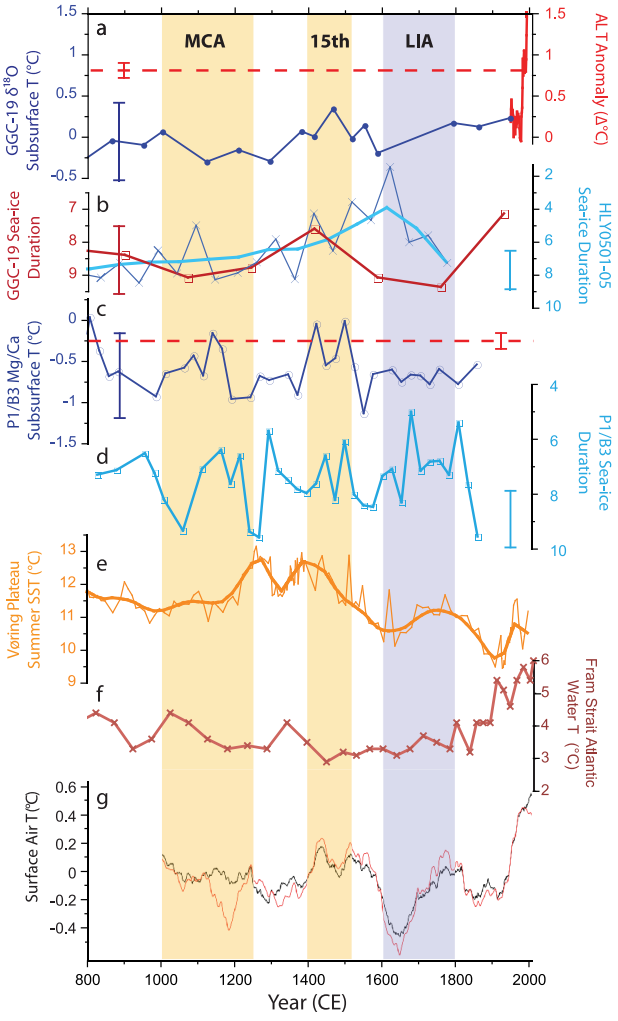

Figure 3. Paleoceanographic variability in the western Arctic over the last 1200 years. (a) The $\delta^{18}O$-based BWT from benthic foraminifer, *I. helenae* in GGC-19, (dark blue) and four-point smooth of normalized instrumental Atlantic Water core temperature anomalies (red line, 1950-2002) [*Polyakov et al.*, 2004]. (b) dinocyst-based sea-ice duration (axis reversed) from GGC-19 (red) and HLY0501-05 (blue, thick line is 3 point smooth) [*McKay et al.*, 2008]. (c) Ostracode Mg/Ca-based BWT and (d) dinocyst-based sea-ice duration [*de Vernal et al.*, 2005] from P1/B3 (axis reversed). (e) The 10m depth summer SSTs in the Norwegian Atlantic Current calculated from the Maximum Likelihood technique on planktic foraminiferal assemblages from the Vøring Plateau [*Andersson et al.*, 2010]; thick line represents a 10-point smooth. (f) Atlantic Water temperature in the Fram Strait reconstructed from planktic foraminiferal assemblages [*Spielhagen et al.*, 2011]. (g) Mean Arctic surface temperature anomalies from terrestrial proxies (red line) and LOVECLIM 1.1 model simulation using proxy data assimilation (black) [*Crespin et al.*, 2009]. Colored bars in Figures 3a–3d represent ± error ranges for proxies in this study. Red dashed line in Figures 3a and 3c is the recorded *in situ* temperature reached at the depth of GGC-19 and P1/B3 during the WTA [from *McLaughlin et al.*, 2009]. Generalized chronology of Northern Hemisphere climatic intervals (MCA = Medieval Climate Anomaly, 15th = 15th Century, LIA = Little Ice Age) is denoted at the top, with warmer intervals shaded in orange and cooler in purple.

noteworthy that anomalous 20th century warming attributed to an amplified high-latitude response to anthropogenic forcing is observed in Arctic terrestrial records of surface atmospheric temperature [*Kaufman et al.*, 2009], model simulations of Arctic climate [*Mann et al.*, 2008], and marine records from the Fram Strait area [*Spielhagen et al.*, 2011]. Although additional paleoceanographic records are needed, our δ^{18}O, Mg/Ca and dinocyst results also suggest that recent temperature excursions in the Atlantic Layer in the western Arctic Ocean are anomalously warm compared to the last millennium.

[11] **Acknowledgments.** We are thankful for the assistance of E. Roosen with core sampling, E. Tappa for stable isotope analyses, L. Gemery, R. Poirier, and R. Glazer with laboratory procedures, M. Henry and B. Fréchette for dinocyst analyses, consultations with L. Polyak and D. Darby, and insightful comments from R. Spielhagen, M. Pavich, M. Robinson, and an anonymous reviewer that greatly improved the manuscript. J.R.F., T.M.C., and R.C.T. thank support by USGS Global Change Program, G.S.D. thanks support from the USGS Global Change Program and the NSF Office of Polar Programs, A.d.V. thanks support by Fond québécois de la recherché sur la nature et les technologies (FQRNT) and the Ministere du Développement économique, innovation et exportation (MDEIE) of Quebec.

[12] The Editor wishes to thank Robert Spielhagen and an anonymous reviewer for their assistance evaluating this paper.

References

Andersson, C., F. S. R. Pausata, E. Jansen, B. Risebrobakken, and R. J. Telford (2010), Holocene trends in the foraminifer record from the Norwegian Sea and the North Atlantic Ocean, *Clim. Past*, *6*, 179–193, doi:10.5194/cp-6-179-2010.

Comiso, J. C., C. L. Parkinson, R. Gersten, and L. Stock (2008), Accelerated decline in the Arctic sea ice cover, *Geophys. Res. Lett.*, *35*, L01703, doi:10.1029/2007GL031972.

Crespin, E., H. Goosse, T. Fichefet, and M. E. Mann (2009), The 15th century Arctic warming in coupled model simulations with data assimilation, *Clim. Past*, *5*, 389–401, doi:10.5194/cp-5-389-2009.

Cronin, T. M., G. S. Dwyer, P. A. Baker, J. Rodriguez-Lazaro, and W. M. Briggs Jr. (1996), Deep-sea ostracode shell chemistry (Mg:Ca ratios) and late Quaternary Arctic Ocean history, in *Late Quaternary Paleoceanography of North Atlantic Margins*, edited by J. T. Andrews et al., *Geol. Soc. Spec. Publ.*, *111*, 117–134.

Cronin, T. M., L. Gemery, W. M. Briggs Jr., M. Jakobsson, L. Polyak, and E. M. Brouwers (2010), Quaternary sea-ice history in the Arctic Ocean based on a new ostracode sea-ice proxy, *Quat. Sci. Rev.*, *29*, 3415–3429, doi:10.1016/j.quascirev.2010.05.024.

Darby, D. A., J. Ortiz, L. Polyak, S. Lund, M. Jakobsson, and R. A. Woodgate (2009), The role of currents and sea ice in both slowly deposited central Arctic and rapidly deposited Chukchi-Alaskan margin sediments, *Global Planet. Change*, *68*, 58–72, doi:10.1016/j.gloplacha.2009.02.007.

de Vernal, A., C. Hillaire-Marcel, and D. A. Darby (2005), Variability of sea ice cover in the Chukchi Sea (western Arctic Ocean) during the Holocene, *Paleoceanography*, *20*, PA4018, doi:10.1029/2005PA001157.

de Vernal, A., C. Hillaire-Marcel, S. Solignac, T. Radi, and A. Rochon (2008), Reconstructing sea ice conditions in the Arctic and sub-Arctic prior to human observations, in *Arctic Sea Ice Decline: Observations, Projections, Mechanisms, and Implications*, *Geophys. Monogr. Ser.*, vol. 180, edited by E. T. DeWeaver et al., pp. 27–45, AGU, Washington, D. C., doi:10.1029/180GM04.

Duplessy, J.-C., E. Ivanova, I. Murdmaa, M. Paterne, and L. Labeyrie (2001), Holocene paleoceanography of the northern Barents Sea and variations of the northward heat transport by the Atlantic Ocean, *Boreas*, *30*, 2–16, doi:10.1080/030094801300062220.

Dwyer, G. S., T. M. Cronin, and P. A. Baker (2002), Trace elements in ostracodes, in *Applications of the Ostracoda to Quaternary Research*, *Geophys. Monogr. Ser.*, vol. 131, edited by J. A. Holmes and A. R. Chivas, pp. 205–225, AGU, Washington, D. C., doi:10.1029/131GM11.

Hald, M., C. Andersson, H. Ebbesen, E. Jansen, D. Klitgaard-Kristensen, B. Risebrobakken, G. R. Salomonsen, M. Sarnthein, H. P. Sejrup, and R. J. Telford (2007), Variations in temperature and extent of Atlantic Water in the northern North Atlantic during the Holocene, *Quat. Sci. Rev.*, *26*, 3423–3440, doi:10.1016/j.quascirev.2007.10.005.

Kaufman, D. S., D. P. Schneider, N. P. McKay, C. M. Ammann, R. S. Bradley, K. R. Briffa, G. H. Miller, B. L. Otto-Bliesner, J. T. Overpeck, and B. M. Vinther (2009), Recent warming reverses long-term Arctic cooling, *Science*, *325*, 1236–1239, doi:10.1126/science.1173983.

Keigwin, L. D., J. P. Donnelly, M. S. Cook, N. W. Driscoll, and J. Brigham-Grette (2006), Rapid sea-level rise and Holocene climate in the Chukchi Sea, *Geology*, *34*(10), 861–864, doi:10.1130/G22712.1.

Lubinski, D. J., L. Polyak, and S. L. Forman (2001), Freshwater and Atlantic water inflows to the deep northern Barents and Kara Seas since ca 13 ^{14}C ka: Foraminifera and stable isotopes, *Quat. Sci. Rev.*, *20*, 1851–1879, doi:10.1016/S0277-3791(01)00016-6.

Mann, M. E., Z. Zhang, M. K. Hughes, R. S. Bradley, S. K. Miller, S. Rutherford, and F. Ni (2008), Proxy-based reconstructions of hemispheric and global surface temperature variations over the past two millennia, *Proc. Natl. Acad. Sci. U. S. A.*, *105*(36), 13,252–13,257, doi:10.1073/pnas.0805721105.

McKay, J. L., A. de Vernal, C. Hillaire-Marcel, C. Not, L. Polyak, and D. Darby (2008), Holocene fluctuations in Arctic sea-ice cover: Dinocyst-based reconstructions for the eastern Chukchi Sea, *Can. J. Earth Sci.*, *45*, 1377–1397, doi:10.1139/E08-046.

McLaughlin, F. A., E. C. Carmack, W. J. Williams, S. Zimmermann, K. Shimada, and M. Itoh (2009), Joint effects of boundary currents and thermohaline intrusions on the warming of Atlantic water in the Canada Basin, 1993–2007, *J. Geophys. Res.*, *114*, C00A12, doi:10.1029/2008JC005001.

Münchow, A., and E. C. Carmack (1997), Synoptic flow and density observations near an Arctic shelf break, *J. Phys. Oceanogr.*, *27*, 1402–1419, doi:10.1175/1520-0485(1997)027<1402:SFADON>2.0.CO;2.

Overland, J. E., M. C. Spillane, D. B. Percival, M. Wang, and H. O. Mofjeld (2004), Seasonal and regional variation of pan-Arctic surface air temperature over the instrumental record, *J. Clim.*, *17*, 3263–3282, doi:10.1175/1520-0442(2004)017<3263:SARVOP>2.0.CO;2.

Polyak, L., et al. (2009), Late Quaternary stratigraphy and sedimentation patterns in the western Arctic Ocean, *Global Planet. Change*, *68*, 5–17, doi:10.1016/j.gloplacha.2009.03.014.

Polyakov, I. V., G. V. Alekseev, L. A. Timokhov, U. S. Bhatt, R. L. Colony, H. L. Simmons, D. Walsh, J. E. Walsh, and V. F. Zakharov (2004), Variability of the intermediate Atlantic water of the Arctic Ocean over the last 100 years, *J. Clim.*, *17*, 4485–4497, doi:10.1175/JCLI-3224.1.

Polyakov, I. V., et al. (2011), Fate of early 2000s Arctic warm pulse, *Bull. Am. Meteorol. Soc.*, *92*, 561–566, doi:10.1175/2010BAMS2921.1.

Risebrobakken, B., M. Moros, E. V. Ivanova, N. Chistyakova, and R. Rosenberg (2010), Climate and oceanographic variability in the SW Barents Sea during the Holocene, *Holocene*, *20*, 609–621, doi:10.1177/0959683609356586.

Rudels, B., E. P. Jones, U. Schauer, and P. Eriksson (2004), Atlantic sources of the Arctic Ocean surface and halocline waters, *Polar Res.*, *23*(2), 181–208, doi:10.1111/j.1751-8369.2004.tb00007.x.

Shackleton, N. J. (1974), Attainment of isotopic equilibrium between ocean water and the benthonic foraminifera *Uvigerina*: Isotopic changes in the ocean during the last glacial, *Colloq. CNRS 219*, pp. 203–210, Cent. Natl. de la Rech. Sci., Paris.

Shimada, K., F. McLaughlin, E. Carmack, A. Proshutinsky, S. Nishino, and M. Itoh (2004), Penetration of the 1990s warm temperature anomaly of Atlantic water in the Canada Basin, *Geophys. Res. Lett.*, *31*, L20301, doi:10.1029/2004GL020860.

Spielhagen, R. F., K. Werner, S. A. Sørensen, K. Zamelczyk, E. Kandiano, G. Budeus, K. Husum, T. M. Marchitto, and M. Hald (2011), Enhanced modern heat transfer to the Arctic by warm Atlantic water, *Science*, *331*, 450–453, doi:10.1126/science.1197397.

Swift, J. H., K. Aagaard, L. Timokhov, and E. G. Nikiforov (2005), Long-term variability of Arctic Ocean waters: Evidence from a reanalysis of the EWG data set, *J. Geophys. Res.*, *110*, C03012, doi:10.1029/2004JC002312.

Weingartner, T. J., D. J. Cavalieri, K. Aagaard, and Y. Sasaki (1998), Circulation, dense water formation, and outflow on the northeast Chukchi shelf, *J. Geophys. Res.*, *103*(C4), 7647–7661, doi:10.1029/98JC00374.

Woodgate, R. A., K. Aagaard, J. H. Swift, K. K. Falkner, and W. M. Smethie (2005), Pacific ventilation of the Arctic Ocean's lower halocline by upwelling and diapycnal mixing over the continental margin, *Geophys. Res. Lett.*, *32*, L18609, doi:10.1029/2005GL023999.

T. M. Cronin, U.S. Geological Survey, 12201 Sunrise Valley Dr., MS926A, Reston, VA 20192, USA.

A. de Vernal, GEOTOP-UQAM-McGill, CP 8888, succ. Centre-Ville, Montréal, Québec H3C 3P8, Canada.

G. S. Dwyer, Division of Earth and Ocean Sciences, Nicholas School of the Environment, Duke University, Durham, NC 27708, USA.

J. R. Farmer, Lamont-Doherty Earth Observatory, Earth Institute at Columbia University, 61 Route 9W, Palisades, NY 10964, USA. (jfarmer@ldeo.columbia.edu)

L. D. Keigwin, Woods Hole Oceanographic Institution, 266 Woods Hole Rd., MS 08, Woods Hole, MA 02543, USA.

R. C. Thunell, Department of Earth and Ocean Sciences, University of South Carolina, 700 Sumter St., Columbia, SC 29208, USA.